

## Direct 3D Imaging of $\text{Al}_{70.4}\text{Pd}_{21}\text{Mn}_{8.6}$ Quasicrystal Local Atomic Structure by X-ray Holography

S. Marchesini,<sup>1,\*</sup> F. Schmithüsen,<sup>2</sup> M. Tegze,<sup>3</sup> G. Faigel,<sup>3</sup> Y. Calvayrac,<sup>4</sup> M. Belakhovsky,<sup>1</sup>  
J. Chevrier,<sup>5</sup> and A. S. Simionovici<sup>2</sup>

<sup>1</sup>*Service de Physique des Matériaux et Microstructures, Département de Recherche Fondamentale sur la Matière Condensée, CEA Grenoble, 17 rue des Martyrs, F-38054 Grenoble, France*

<sup>2</sup>*ESRF, BP 220, F-38043 Grenoble Cedex, France*

<sup>3</sup>*Research Institute for Solid State Physics and Optics, H-1525 Budapest, POB 49, Hungary*

<sup>4</sup>*C.E.C.M.\_C.N.R.S., 15, rue G. Urbain, F-94407 Vitry CEDEX, France*

<sup>5</sup>*LEPES CNRS Grenoble, BP 166, 38042 Grenoble cedex 9, France*

(Received 13 June 2000)

Inverse x-ray fluorescence holography was used to explore the local atomic order of a nearly perfect quasicrystal with composition  $\text{Al}_{70.4}\text{Pd}_{21}\text{Mn}_{8.6}$ . We have demonstrated the possibility of direct 3D imaging of the atomic decoration in a quasicrystal. We have obtained the average 3D environment of selected coordination shells around the Mn atoms. These results open the way to obtaining further and more complete information about the various coordination shells in complex materials by measuring multiple energy x-ray holograms at different sites.

PACS numbers: 61.44.Br, 42.40.-i, 61.10.-i

Besides the crystalline and amorphous solids, the quasicrystals are a new type of space filling form of matter. These intermetallic compounds are stable and exhibit a specific long range order together with an orientational order associated with symmetry properties which are forbidden in periodic crystals [1]. Among quasicrystals the icosahedral AlPdMn system is considered as a model system [2]. For this system, fivefold axes are observed in diffraction patterns obtained using neutron [3], x-ray [3,4], or electron beams [5–7]. These diffraction data are the experimental basis of the accepted models, which describe the atomic decoration of the quasicrystalline structure [3,8]. In fact, for all discovered quasiperiodic structures, determination of atomic decoration remains a central issue. Recently, high resolution electron microscopy images [9,10] of the 2D AlNiCo quasiperiodic structures have been quantitatively analyzed using a single 2D decorated cluster of atoms [11].

In general, the structure of nonperiodic systems like amorphous materials cannot be exactly described by a finite set of parameters. A striking feature of quasicrystals is that in spite of the fact that they are also nonperiodic in 3D space, their structure can still be characterized by a minimal set of parameters in the six-dimensional superspace, similar to “normal” crystals in 3D real space. This periodic 6D structure can be projected on 3D space to obtain a perfect idealized quasicrystalline structure [2,12,13]. Starting from these models, one obtains not only long range order but also evidence for a high local order with respect to distances and orientations. In particular, this description implies a finite set of local atomic structures around the Mn atoms.

Hard x-ray holography using an inside reference point is a local method capable of imaging the environment of selected atoms in 3D with no *a priori* model [14]. The capa-

bilities of this method have been demonstrated in previous experiments [15–20]. In the last few years the technique has been developed to a level that makes its application practical. The measuring time was decreased to the hour range, and the real space resolution was significantly improved [18], both in absolute value and in directionality. The high statistical accuracy and the rigorous control of experimental conditions allowed even the imaging of light atoms [21]. Up to now x-ray holography has been used in model crystals with simple atomic decoration.

The combination of x-ray holography with quasicrystals opens two unique experimental opportunities. First, we can demonstrate the efficiency of this new technique in the case of a complicated structure with different local environments. For the first time x-ray holography can be tested on a noncrystalline solid. Second, this experiment can directly visualize the average neighborhood of one type of atom (Al, Pd, or Mn). This will be the first time that the atomic positions in quasicrystals can be observed in direct space and in 3D with no prerequisite atomic model and no necessity for a sophisticated extension of the classical crystallography to a six-dimensional space.

In spite of the above improvements in the technique, the measurement of quasicrystals is not without difficulties. In the following we outline the most important problems. First, holography needs, at the present technical stage, a large flat sample in which, besides the short range order, there is also orientational order. Nowadays, the growth technique of quasicrystals is perfected to a level that large ideal quasicrystals could be produced [22]. Their superb quality was proven by the observation of dynamic effects such as the Bormann effect [23] or the fine structure of x-ray standing wave lines (XSWL) [24,25]. The orientational order is an inherent property of the quasicrystals. However, in these samples selected atoms can have

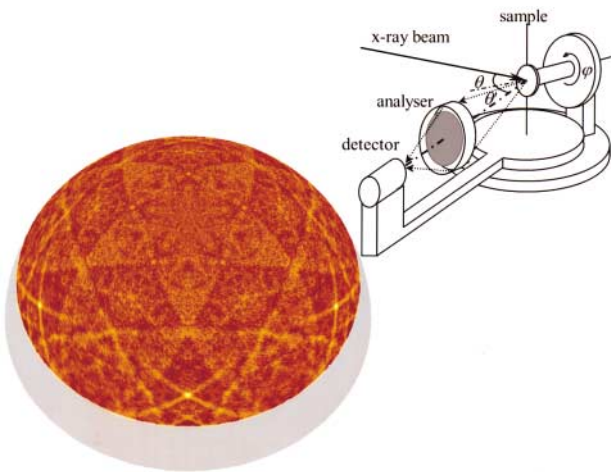


FIG. 1 (color). Mn fluorescence versus incident beam direction. The gray part corresponds to the range of  $\theta$  angle inaccessible due to practical constraints. The inset is a sketch of our experimental setup.

neighbors not in a single but in a few distinct orientations. Since in the hologram all the possible orientations appear at the same time, the separation of these require additional information. This can be obtained from chemical considerations or from comparing the experimental data to existing models. The second problem is connected to the diffraction peaks, which densely fill the reciprocal space down to low  $Q$  values. Two sources of these photons can be distinguished: (i) elastic scattering of the incident beam (normal Bragg scattering) and (ii) elastic scattering of the fluorescent radiation excited by the incident beam (Kossel lines) [26,27]. Since the intensity of both of these is much larger than that of the holographic signal, they have to be removed. The first one can be filtered out by a crystal analyzer placed before the detector and set to the fluorescent energy of the central atom. The Kossel lines are sharp and do not contribute to the low spatial frequency component of the hologram [28].

After discussing the special problems connected to holographic imaging of quasicrystals, we briefly describe the experimental conditions. The  $\text{Al}_{70.4}\text{Pd}_{21}\text{Mn}_{8.6}$  icosahedral quasicrystal sample was grown by the Czochralski method. A 20 mm diameter circular wafer with 1 mm thickness was cut from the bulk. The orientation of its large flat surface was chosen to be perpendicular to a fivefold axis. The experiments were done at the ID22 undulator beam line of ESRF. The experimental setup was a slightly modified version of the one used in our earlier measurements [29]. There were two independent vertical coaxial rotations ( $\theta, \theta'$ ) and a horizontal one ( $\varphi$ ) holding the sample with its large flat surface perpendicular to this axis (see inset of Fig. 1). The changes included the analyzer crystal and mechanical drivers [29]. The diameter of the “crystal analyzer ribbon” was decreased, which allowed the use of a more compact mechanics. This led to higher stability and a shorter beam path reducing the air absorption. Therefore

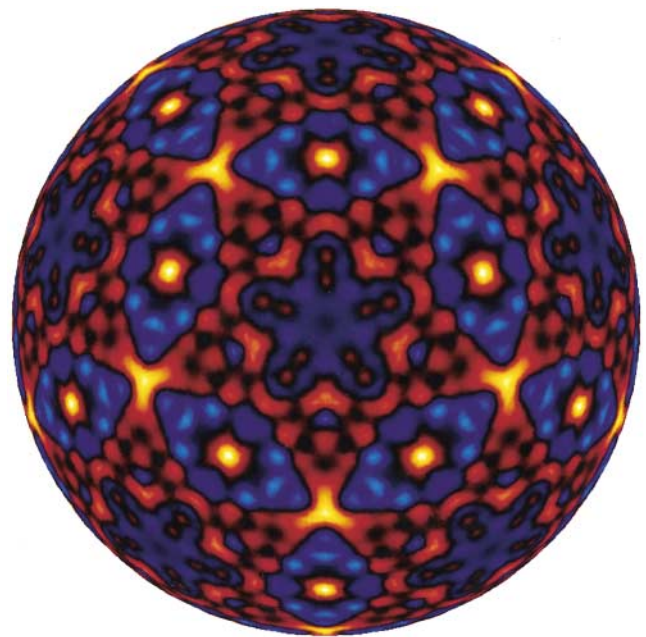


FIG. 2 (color). The hologram around the Mn atoms. It has been obtained by first, extending the data of Fig. 1 to the full solid angle based only on the symmetries of these data (i.e., only intrinsic information has been used), and second, removing the standing wave pattern by low frequency filtering.

we could avoid the He beam path even at low fluorescent energies (as  $\text{Mn } K_{\alpha} = 5.89 \text{ keV}$ ). The energy of the incident beam was 16 keV with a bandwidth of about 2 eV. Data were collected in the so-called inverse mode [16,17] in which the atoms serve as detectors of the interference field of the direct and scattered waves. The Mn atoms were chosen as reference points.

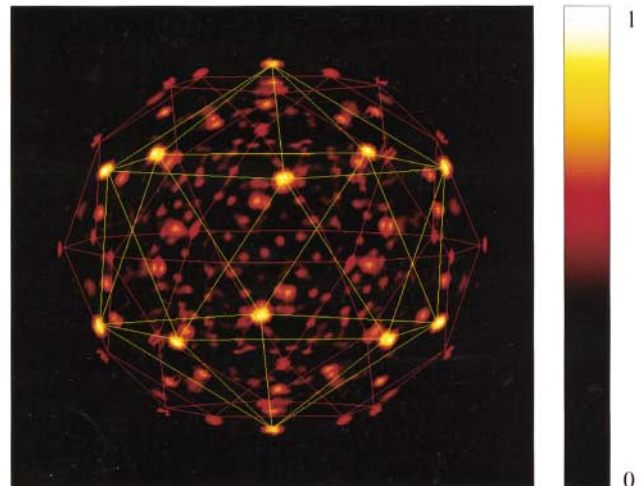


FIG. 3 (color). Real part of the reconstructed wave field. The bright yellow spots represent the atomic positions. Other small intensity spots might come from other atoms or they are artifacts intrinsic to the single energy reconstruction. Further experimental data are required to sort out these features. The yellow lines connect the most intense atomic sites of the model.

The intensity variation of the Mn fluorescence is shown in Fig. 1 as a function of the incident beam direction. The number of photons was measured up to  $\theta = 70^\circ$  (see inset of Fig. 1 for definition of the angles). The rough data were normalized with the incident beam monitor, corrected for the flat specimen absorption [17]. The image clearly shows the fivefold symmetry and also several threefold axes and mirror planes characteristic of the generalized crystallographic group of the icosahedral quasicrystal ( $Pm\bar{3}5$ ). Sharp lines are also visible; they can be identified as the x-ray standing wave line pattern. In principle, reconstruction could be done at this point. However, one cannot expect a good quality 3D image of atoms. The cause of it is that a substantial part of the hologram could not be measured because of the flat specimen geometry [18]. The missing information (see gray part in Fig. 1) causes spurious oscillation and a strongly degraded resolution in the direction perpendicular to the crystal surface [17]. This would result in the appearance of high intensity spots even at those places where atoms are not expected. To circumvent this problem, the effect of the missing part has to be compensated. This was done by extending the experimental data to the full sphere using the symmetry elements found in the measurement itself [17]. The result is shown in Fig. 2. We applied the Helmholtz-Kirchhoff integral transform on this hologram. The real space reconstruction is depicted in Fig. 3. The interpretation of this picture is not as trivial as the interpretation of the results in the case of normal crystals. Therefore a more detailed discussion is appropriate here. Two features are striking at first sight: (i) The twelve highest intensity spots are located in the corner of an icosahedron. (ii) The distance of these spots from the central atom is about 4.6 Å. It is clear from considerations on the chemistry and the material density that these points cannot be the first atomic neighbors. The question arises: How is it possible? In all fluorescence x-ray holography experiments done so far, first neighbors could be seen, and usually they had the highest intensity. In order to understand these observations, we turn to models of the atomic decoration of this quasicrystal [3]. We tabu-

lated the atoms according to their distance from the Mn atoms (see Table I). The most important characteristics, such as the number of sites, the type of atoms, and the weighted occupation of the different coordination shells are also shown. We can use this table to estimate the visibility of atoms in the reconstructed real space image. In inside source holography the expected weight of an atom is proportional to  $(f(\theta)/r)^2$ . Here  $r$  stands for the distance from the central atom and  $f(\theta)$  for the average scattering factor of the site under question. In first approximation  $f(\theta) \sim \sum z_i^* p_i$ , where  $z_i$  and  $p_i$  are the atomic number and partial occupation of component "i," respectively.

Taking into account the values in Table I, it is clear that the highest intensity spots are a combination of the 5th coordination shell of Pd, the third of Al, and the first of Mn. According to the table, we should also see 30 sites at 4.8 Å with 25% reduced intensity (see the red lines in Fig. 3). However, these spots are not easily recognized. This is explained by the cancellation of the real and twin images, which depends on the distance of the object from the central atom and the wavelength of the hologram-forming wave [15,16]. In our case this effect reduces the intensity of the atoms in the 6th coordination shell to about one-sixth of that of the 5th one. Therefore the atoms of the 6th shell cannot be clearly imaged at the present statistical level of the measurements. Further, it is interesting to note that closer shells are much less occupied, and as a consequence they cannot be seen at all. These findings are the first direct evidence, which experimentally gives the average 3D atomic decoration for selected shells. The results are in good agreement with well established models of quasicrystal structure [3,7].

This experiment opens the way to the application of atomic resolution holography to solids with orientational order in the absence of periodicity. Furthermore, x-ray holography is still efficient in the presence of a high mosaicity, which affects the alignment of symmetry axis from place to place in solids. On this basis, new problems can be tackled, such as the first stage of organization of ill ordered matter (proteins, etc.).

TABLE I. Average scattering factor and distances for the first ten atomic shells about the central Mn atoms according to one of the existing models of this quasicrystal [3].

Coordination shell	Number of sites	Distance (Å)	Elements	$\sum z_i^* p_i$
1	20	2.57	Al <sub>1</sub> + Pd <sub>1</sub>	4.98
2	12	2.82	Pd <sub>2</sub>	0.18
3	30	2.96	Al <sub>2</sub> + Pd <sub>3</sub>	2.12
4	20	4.15	Pd <sub>4</sub>	2.48
5	12	4.56	Al <sub>3</sub> + Mn <sub>1</sub> + Pd <sub>5</sub>	20.53
6	30	4.80	Al <sub>4</sub> + Mn <sub>2</sub> + Pd <sub>6</sub>	18.78
7	60	5.44	Al <sub>5</sub>	1.04
8	60	5.64	Al <sub>6</sub>	0.16
9	12	5.64	Al <sub>7</sub>	0.013
10	60	6.62	Al <sub>8</sub> + Mn <sub>3</sub> + Pd <sub>7</sub>	10.24

To conclude, we point out future possibilities. Although the imaging of the local atomic environment in quasicrystals is among the first applications of hard x-ray holography, the result clearly shows the power of this method. It gives structural information in direct space without presuming a prerequisite model. This cannot be directly obtained by other techniques. With further improvements of the experimental conditions and evaluation procedure the continuation of these experiments will lead to definite improvements of our knowledge on the local structure and defects in quasicrystals. Indeed, collection of data at many energies would extend the range of imaging, and we could show evidences for the inflation properties, or define more precisely atomic environments in the first 5–6 coordination shells. An extended analysis by comparing the experimental data with the  $\sum z_i^* p_i$  values further ascertains the validity of the different models. These will contribute significantly to the understanding of the quasicrystals. Ultimately the mapping of 3D atomic decorations in various types of these fascinating materials becomes reality.

The authors thank the ESRF and, in particular, the ID22 staff members for their help during the experimental work. We are pleased to acknowledge the careful critical reading and useful remarks about the quasicrystal models from Christian Janot and Marc de Boissieu. This work was supported by EC Grant No. ERBFMBICT961366 (S.M. Marie-Curie Fellowship), OTKA 022041, BIO-4CT98-0377, and OMFB 02264/98 (G. F. and M. T.).

---

\*Present address: Materials Sciences Division, Lawrence Berkeley National Laboratory, Berkeley, CA 94720.

- [1] D. Shechtman, I. Blech, D. Gratias, and J. W. Cahn, *Phys. Rev. Lett.* **53**, 1951 (1984).
- [2] C. Janot, *Quasicrystals: A Primer* (Oxford Science Publications, Oxford, 1992).
- [3] M. Boudard, M. de Boissieu, C. Janot, G. Heger, C. Beeli, H. U. Nissen, H. Vincent, R. Ibberson, M. Audier, and J. M. Dubois, *J. Phys. Condens. Matter* **4**, 10 149 (1992).
- [4] C. Janot, M. de Boissieu, M. Boudard, H. Vincent, M. Durand, J. M. Dubois, and C. Dong, *J. Non-Cryst. Solids* **150**, 322 (1992).
- [5] M. Audier, M. Durand-Charre, and M. de Boissieu, *Philos. Mag. B* **68**, 607 (1993).
- [6] A. P. Tsai, Y. Yokoyama, A. Inoue, and T. Masumoto, *J. Non-Cryst. Solids* **150**, 327 (1992).
- [7] D. Naumovic *et al.*, *Surf. Sci.* **433-435**, 302–306 (1999); *Phys. Rev. B* **60**, R16 330–R16 333 (1999).
- [8] A. Katz and D. Gratias, *J. Non-Cryst. Solids* **153&154**, 187 (1993).
- [9] Y. Yan and S. J. Pennycook, *Nature (London)* **403**, 226 (2000).
- [10] K. Tsuda, Y. Nishida, K. Saitoh, M. Tanaka, A. P. Tsai, A. Inoue, and T. Masumoto, *Philos. Mag. A* **74**, 697 (1996).
- [11] P. J. Steinhardt, H.-C. Jeong, K. Saitoh, M. Tanaka, E. Abe, and A. P. Tsai, *Nature (London)* **396**, 55 (1998); *Nature (London)* **399**, 84(E) (1999).
- [12] J. W. Cahn, D. Shechtman, and D. Gratias, *J. Mater. Res.* **1**, 13 (1986).
- [13] M. Cornier-Quiquandon, D. Gratias, and A. Katz, in *Methods of Structural Analysis of Modulated Structures and Quasicrystals, Lekeitio-Bilbao, Spain, 1991*, edited by J. M. Perez-Mato, F. J. Zuniga, and G. Madariaga (World Scientific, Singapore, 1991), p. 313.
- [14] A. Szöke, in *Short Wavelength Coherent Radiation: Generation and Applications*, edited by D. T. Attwood and J. Boker, AIP Conf. Proc. No. 147 (American Institute of Physics, New York, NY, 1986), p. 361.
- [15] M. Tegze and G. Faigel, *Nature (London)* **380**, 49 (1996).
- [16] T. Gog *et al.*, *Phys. Rev. Lett.* **76**, 3132 (1996).
- [17] G. Faigel and M. Tegze, *Rep. Prog. Phys.* **62**, 355 (1999).
- [18] M. Tegze, G. Faigel, S. Marchesini, M. Belakhovsky, and A. I. Chumakov, *Phys. Rev. Lett.* **82**, 4847 (1999).
- [19] S. Marchesini, Ph.D. thesis, Université J. Fourier, Grenoble, France, 2000.
- [20] T. Hiort, D. V. Novikov, E. Kossel, and G. Materlik, *Phys. Rev. B* **61**, R830–R833 (2000).
- [21] M. Tegze, G. Faigel, S. Marchesini, M. Belakhovsky, and O. Ulrich, *Nature (London)* **407**, 38 (2000).
- [22] A. P. Tsai, A. Inoue, and T. Masumoto, *Philos. Mag. Lett.* **62**, 2409 (1990).
- [23] S. W. Kycia, A. I. Goldman, T. A. Lograsso, D. W. Delaney, D. Black, M. Sutton, E. Dufresne, R. Brüning, and B. Rodricks, *Phys. Rev. B* **48**, 3544 (1993).
- [24] T. Jach, Y. Zhang, R. Colella, M. de Boissieu, M. Boudard, A. I. Goldman, T. A. Lograsso, D. W. Delaney, and S. Kycia, *Phys. Rev. Lett.* **82**, 2904 (1999); T. Jach, in *Proceedings of the International Conference on Quasicrystals 7th*, Stuttgart, 1999, edited by H.-R. Trebin and K. Urban [Mater. Sci. Eng. (to be published)].
- [25] G. Cappello, A. Dechelette, F. Schmithüsen, S. Decossas, J. Chevrier, F. Comin, V. Formoso, M. de Boissieu, T. Jach, R. Colella, T. Lograsso, C. Jenks, and D. Delaney, in *Proceedings of the International Conference on Quasicrystals 7th*, Stuttgart, 1999, edited by H.-R. Trebin and K. Urban [Mater. Sci. Eng. (to be published)].
- [26] W. Kossel, V. Loeck, and H. Voges, *Z. Phys.* **94**, 139 (1935).
- [27] In the case of inverse holography an analog to the Kossel lines, the x-ray standing wave line pattern appears.
- [28] M. Tegze and G. Faigel, *Europhys. Lett.* **16**, 41 (1991).
- [29] S. Marchesini, O. Ulrich, G. Faigel, M. Tegze, M. Belakhovsky, and A. I. Simionovici, "Instrumental development of x-ray atomic holography at ESRF," *Nucl. Instrum. Methods Phys. Res., Sect. A* (to be published).